BIOCHEMISTRY

Multicomponent reaction–derived covalent inhibitor space

Fandi Sutanto[1]*, Shabnam Shaabani[1]*, Constantinos G. Neochoritis[2], Tryfon Zarganes-Tzitzikas[1], Pravin Patil[1], Ehsan Ghonchepour[1], Alexander Dömling[1†]

The area of covalent inhibitors is gaining momentum due to recently introduced clinical drugs, but libraries of these compounds are scarce. Multicomponent reaction (MCR) chemistry is well known for its easy access to a very large and diverse chemical space. Here, we show that MCRs are highly suitable to generate libraries of electrophiles based on different scaffolds and three-dimensional shapes and highly compatible with multiple functional groups. According to the building block principle of MCR, acrylamide, acrylic acid ester, sulfurylfluoride, chloroacetic acid amide, nitrile, and α,β-unsaturated sulfonamide warheads can be easily incorporated into many different scaffolds. We show examples of each electrophile on 10 different scaffolds on a preparative scale as well as in a high-throughput synthesis mode on a nanoscale to produce libraries of potential covalent binders in a resource- and time-saving manner. Our operational procedure is simple, mild, and step economical to facilitate future covalent library synthesis.

INTRODUCTION

Covalent inhibitors have a rich tradition as drugs exemplified in the classic and lifesaving β-lactam antibiotics (*1*). More than 25% of approved enzyme targeting drugs work through a covalent mechanism (*2*). Recently, covalent inhibitors have experienced a renaissance, for example, with the clinical introduction of the Bruton's tyrosine kinase inhibitor zanubrutinib or the experimental G12C RAS inhibitor AMG510 (Fig. 1, A and B) (*3*, *4*).

In addition, nature extensively uses the principle of covalent modification exemplified by the tubulin binder cyclostreptin (Fig. 1, A and B) (*5*). Covalent drugs potentially offer several advantages over noncovalent drugs, including increased potency and therefore lower dosing, selectivity, duration of action, and resistance to mutations (*6*). However, covalent drugs have been controversial because of their potential off-target binding leading to unforeseeable, e.g., idiosyncratic or off-target toxicity (*7*). Selectivity issues and side effects could be potentially mitigated by maximizing selectivity of binding to the target protein, maintaining a low dose, and avoiding reactive metabolites (*8*). Outside drug discovery, covalent inhibitors also play an important role as tool compounds in chemical biology to identify ligands in proteome-wide screens (*9*). For example, a chemical proteomic approach has recently led to the discovery of a selective probe for the difficult to target mitochondrial pyruvate carrier complex (*10*). Covalent targeting of kinases based on endogenous or mutated cysteines is also a proven clinical anticancer strategy (*11*). The targets of covalent inhibitors in proteins are the nucleophilic amino acid side chains—mostly cysteine and serine but also threonine, histidine, tyrosine, lysine, arginine, or tryptophan (Fig. 1C). Moreover, aspartate and glutamate have been targeted by covalent modifications (*12*). Typical electrophiles used in covalent inhibitors include acrylamide (*13*), acrylic acid ester, sulfurylfluoride (*14*), boronic acid (*15*), chloroacetic acid amide (*16*), nitrile (*17*), and α,β-unsaturated sulfonamide warheads (Fig. 1C) (*18*). Another cysteine-specific technology is disulfide trapping, which is based on the principle of reversible thiol-disulfide exchange between the protein target and the disulfide containing screening compounds (*19*). Among the different electrophiles, a certain degree of nucleophile selectivity can be reached (*20*). For instance, boronic acid is an oxophile and has a preference for hydroxyl amino acids, while acrylamides are thiophiles and react often with cysteines in a Michael addition. To discover hits and initial leads, screening of diverse libraries based on multiple electrophiles imprinted on multiple scaffolds and decorated with many additional functional groups is desirable. Despite the growing importance of covalent targeting, diverse screening libraries decorated with a range of chemical functionalities are scarce. Past covalent library screening efforts were mostly performed on a small scale (*21*–*23*). Libraries of covalent inhibitors are often synthesized from (commercial) building blocks and additions of an electrophile by late-stage functionalization, e.g., acrylamide (*24*). Moreover, the few commercially available covalent screening libraries are of limited size and diversity.

Here, we introduce the use of multicomponent reaction (MCR) chemistry for the production of unmatched diverse libraries of covalent inhibitors. In combination with newly reported building blocks, our approach circumvents problems ascribed to traditional electrophile library synthesis such as slow sequential synthesis and limited library diversity. We report the synthesis of 10 MCR-compatible and 10 commercially available building blocks that were introduced into 10 different scaffolds to produce 102 compounds with a diverse set of electrophiles. The diversity of warheads included 10 different classes of electrophiles. To satisfy different compound quantity demands, we demonstrated the synthesis on different scales covering four orders of magnitude. Two synthesis protocols were reported in an automated fashion on a nanoscale or on a millimole scale for repeated use of the screening libraries.

[1]Department of Drug Design, University of Groningen, A. Deusinglaan 1, 9700 AD Groningen, The Netherlands. [2]Department of Chemistry, University of Crete, 700 13 Heraklion, Greece.
*These authors contributed equally to this work.
†Corresponding author. Email: a.s.s.domling@rug.nl

RESULTS AND DISCUSSION

Chemistry and design considerations

To design a reactive library, we have to consider the nature of the electrophile, the structure of the noncovalent diversity elements, and

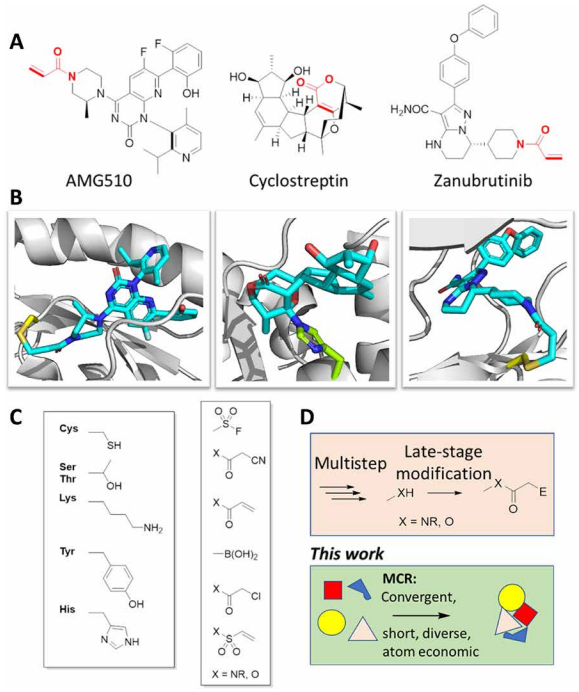

Fig. 1. Covalent inhibitors in medicinal chemistry and natural products. (**A** and **B**) Three compounds covalently binding to their protein targets. AMG510, a G12C RAS inhibitor [Protein Data Bank (PDB) ID: 6OIM], cyclostreptin binding to His^{229} of tubulin (PDB ID: 6QTN), and Bruton's tyrosine kinase inhibitor zanubrutinib (PDB ID: 6J6M). (**C**) Common electrophilic warheads and nucleophilic amino acid targets. (**D**) Synthetic strategies to covalent inhibitors.

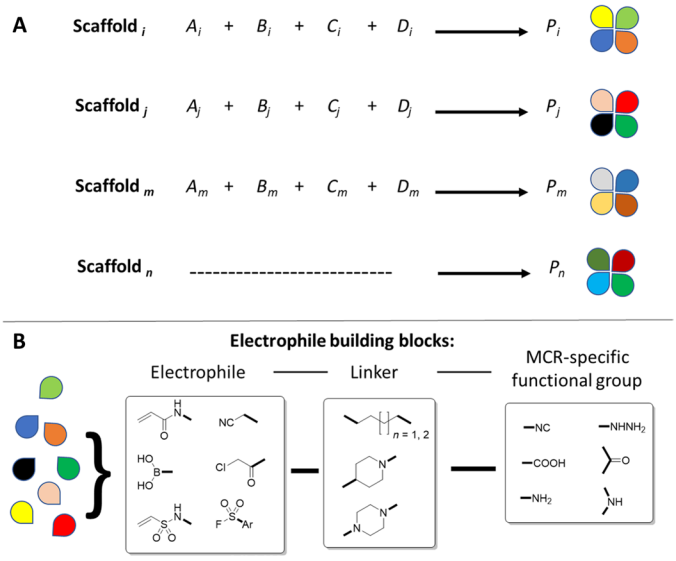

Fig. 2. Design of electrophile libraries. (**A**) The use of multiple MCRs allows for great scaffold diversity. (**B**) The electrophile building blocks consist of three parts: the electrophile functional group, the linker, and the MCR-compatible functional group. The colored forms graphically represent different types of building blocks.

the linker between them. The nature and thus intrinsic reactivity of the electrophile moiety can vary a lot (*20*, *25*, *26*). In our design, the electrophile is often attached to an aliphatic linker, which overall should normalize the intrinsic reactivity of the warhead. The distance between the electrophilic warhead and the diversity element is important because an effective compound must make productive interactions with the protein by displaying the electrophile at the correct distance and orientation to react with the nucleophile residue. The flexibility of the linker element also needs considerations not only to adapt to the shape of the receptor pocket but also to potentially reduce conformational space while improving drug-like properties, e.g., oral bioavailability by increasing membrane permeation. Thus, linker lengths and geometries are important design elements for electrophile libraries. The composition of the linker can also have important effects on the chemical reactivity of the electrophile (*27*). In addition, the nature of the electrophile is of great importance to address specific nucleophilic amino acid side chains and to fine-tune reactivity, e.g., oxophile versus thiophile. Last, the shape and three-dimensional (3D) pharmacophore distribution of ligands encoded in the scaffold is of high importance for noncovalent receptor interaction to provide a negative imprint of the binding pocket. Very few libraries containing a diverse selection of electrophiles, linker elements, scaffolds, and conformational space are available for purchase from commercial vendors, perhaps because of the long-standing bias toward noncovalent binders (*28*, *29*). To create libraries of electrophiles, we used a convergent one-pot MCR approach using an array of available or easily accessible electrophile building blocks. The electrophile moiety was introduced into different kinds of building blocks with an orthogonal functional group required for a variety of different MCRs (Fig. 2). To keep the overall average molecular weight of the target compounds low, we designed rather small electrophile building blocks based on small aliphatic chains or six-membered rings to reflect flexibility and stiffness. However, it should be noted that our choice of linkers is arbitrary and many other building blocks are possible and would not be limited by the chemistry used. Additional considerations in our design were to enrich the library with related analogs to allow preliminary structure-activity relationships to be deduced directly from a primary screen.

To provide a broad range of scaffolds of different shape and 3D pharmacophore distribution, we used 10 different MCRs (Table 1). While hundreds of MCR scaffolds were previously described, we selected a subset to represent a broad range of chemotypes that have been previously used in the discovery of bioactive matter, including semirigid *bis*-amides (a) (*30*), heterocyclic basic α-amino tetrazoles (b) (*31*), heterocyclic planar imidazoles (c) (*32*), hydantoins (d) (*30*, *33*), flexible hydroxyacylcarboxy amides (e) (*34*), bicyclic planar heterocycles (f) (*35*, *36*), heterocyclic nonbasic α-hydroxy tetrazole (g) (*37*, *38*), elongated basic *bis*-amides (h) (*39*), cyclic *bis*-amides with cis conformation (i) (*40*), and heteroaromatic conformationally constrained thiophene carboxamides (j) (*41*).

For the creation of our electrophile libraries, we required specific bifunctional building blocks. The synthesis of each building block was performed on a gram scale (Fig. 3). Primary amine-containing building blocks **6** and **7** are short and rather flexible aliphatic diamine-derived mono acylates with two and three rotatable bonds (nrb), respectively. Acrylate **10** features an acyl hydrazine moiety. Piperidines **14** and **24** are cyclic motifs featuring a vinyl sulfonamide and an acrylamide warhead along with a secondary amine and ketone as an MCR-compatible functional group, respectively. β-Cyanoethyl isocyanide **18** featuring a soft nitrile electrophile was synthesized (*42*). A flexible (nrb = 2) ethylenediamine-derived mono isocyanide

Table 1. The MCRs used to create libraries with electrophilic moieties. The different scaffolds are boxed in different colors that will be used throughout the manuscript.

Entry	Reaction Scheme	Reaction Name
a	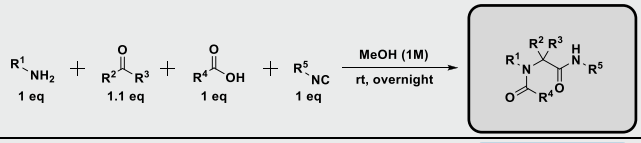	Ugi Four-Component Reaction (U-4CR)
b	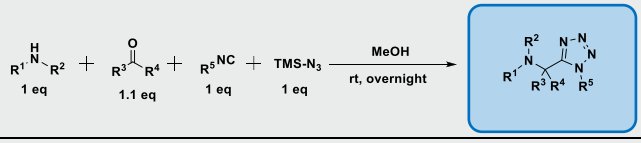	Ugi Tetrazole Reaction (UT-4CR)
c	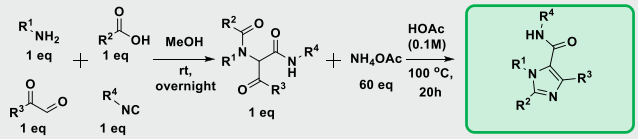	Ugi-Imidazole Reaction (UI-4CR)
d	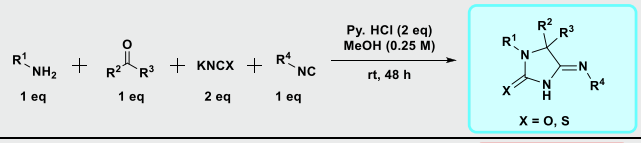	Ugi-Hydantoin Reaction (UH-4CR)
e	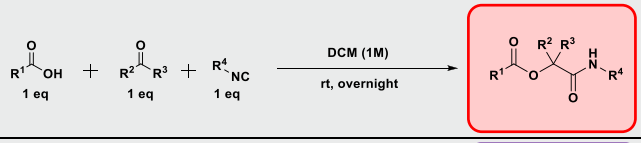	Passerini Three-Component Reaction (P-3CR)
f	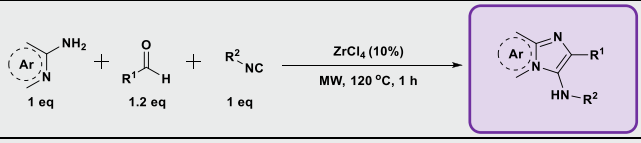	Groebke-Blackburn-Bienaymé Reaction (GBB-3CR)
g	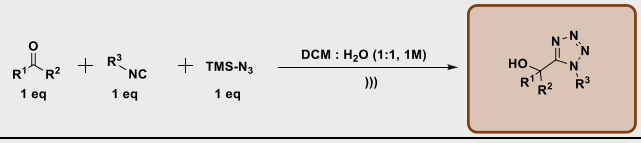	Passerini Tetrazole (PT-3CR)
h	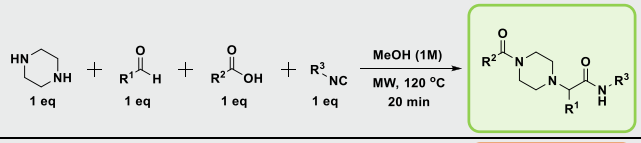	Split Ugi Four-Component Reaction (SU-4CR)
i		Joullié-Ugi Three-Component Reaction (JU-3CR)
j	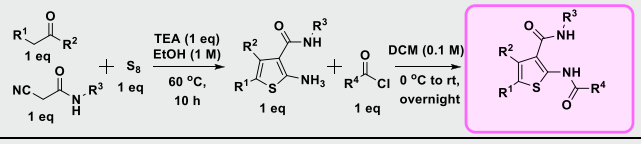	Gewald Three-Component Reaction and acylation (GW-3CR)

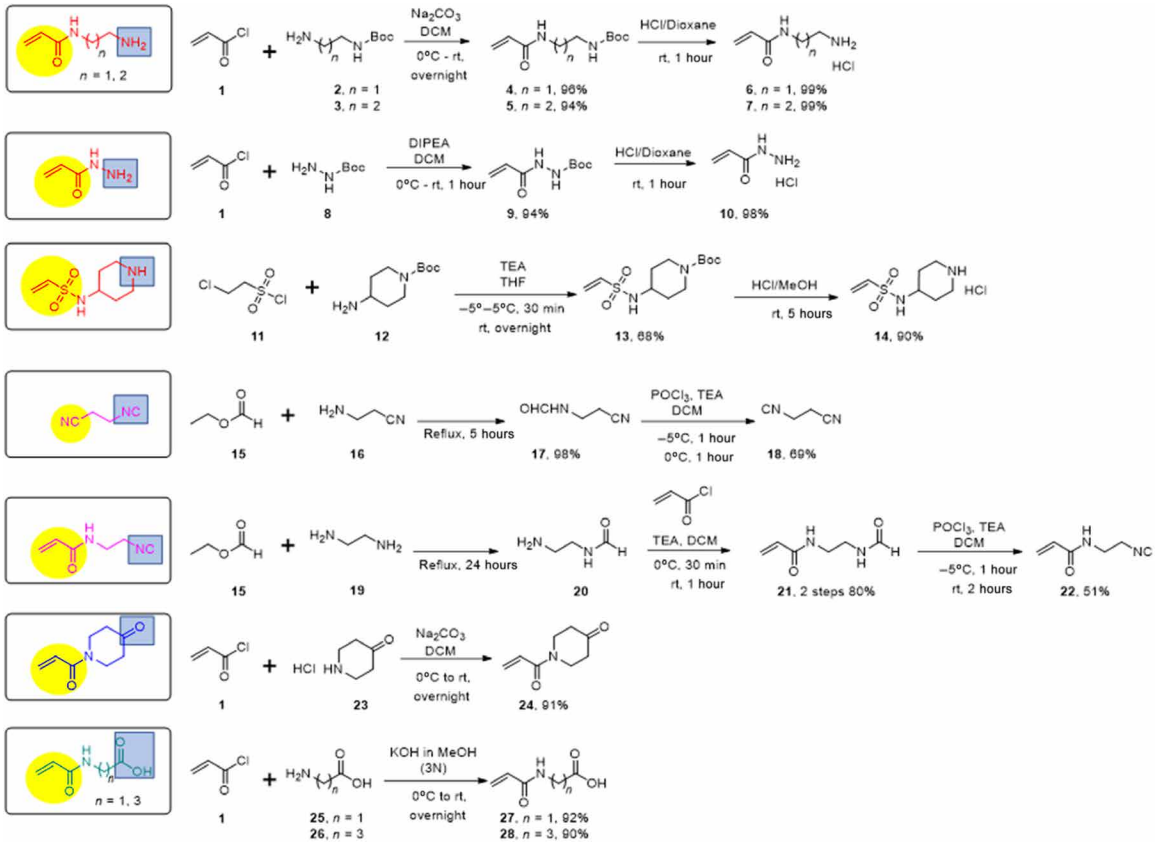

Fig. 3. Synthesis of specific bifunctional electrophile building blocks. The electrophile and the MCR functional groups are marked in yellow and blue, respectively. rt, room temperature.

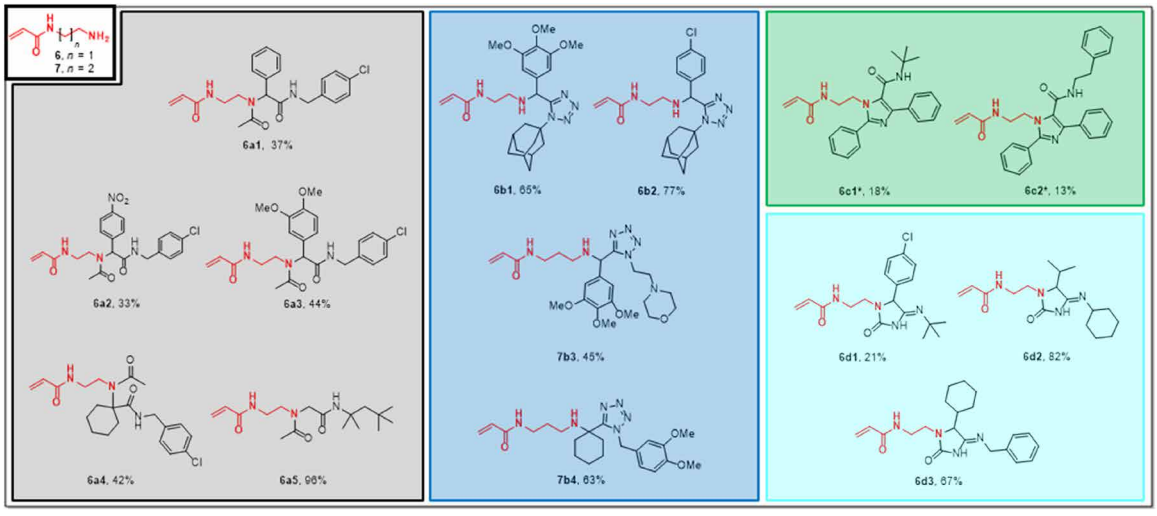

Fig. 4. Millimole-scale synthesis of electrophiles based on acrylamide amine building blocks 6 and 7. (*yield over two steps). The color of the boxes refers to the scaffolds shown in Table 1.

mono acrylamide **22** was accessed by a short three-step sequence. Last, acrylamide carboxylic acids **27** and **28** were produced with two different short-length linkers. Moreover, additional building blocks were used, such as unsubstituted and differentially substituted acrylic acids **29** to **32** (Fig. 7), chloroacetic acid **33**, and chloroacetyl chloride **1** and 2-butynoic acid **35** (Fig. 8). The but-2-ynamide electrophile has been used recently in the discovery of the covalent Bruton's tyrosine kinase inhibitor branebrutinib as a superior electrophile over acrylamides and vinyl sulfonamides (*43*).

To show the feasibility of creating complex electrophiles as potential covalent binders, we performed model reactions for each scaffold using a selection of electrophile building blocks (Figs. 4 to

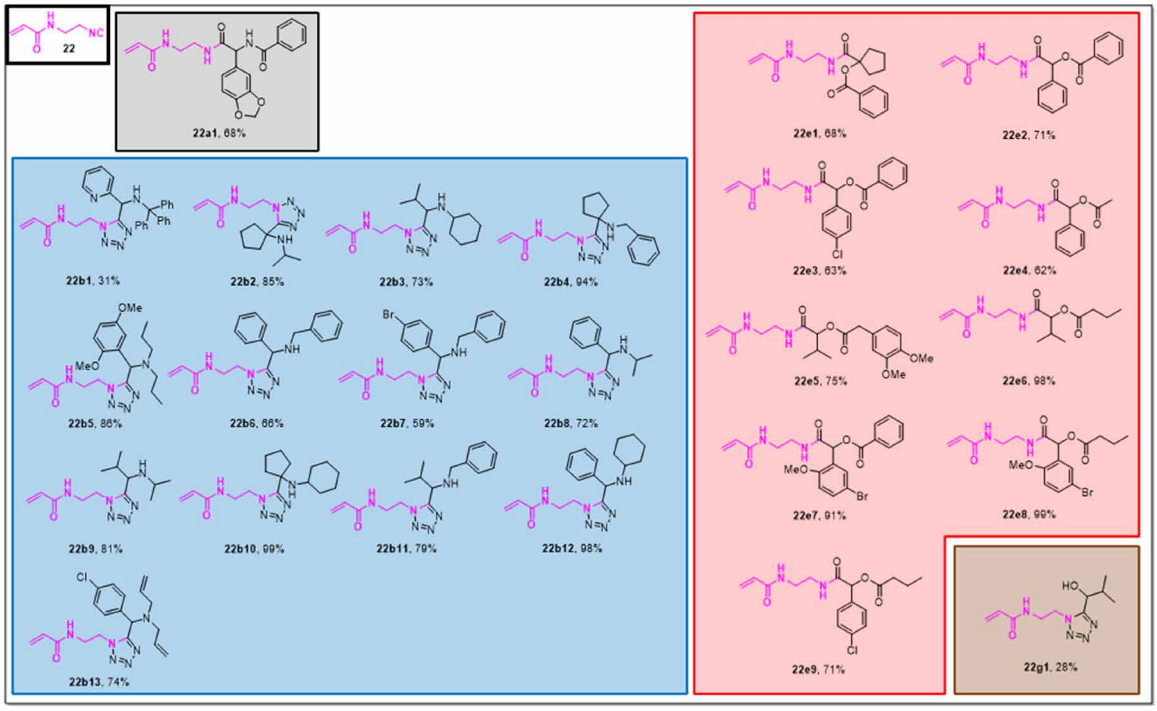

Fig. 5. Millimole-scale synthesis of electrophiles based on acrylamide isocyanide building block 25. The color of the boxes refers to the scaffolds shown in Table 1.

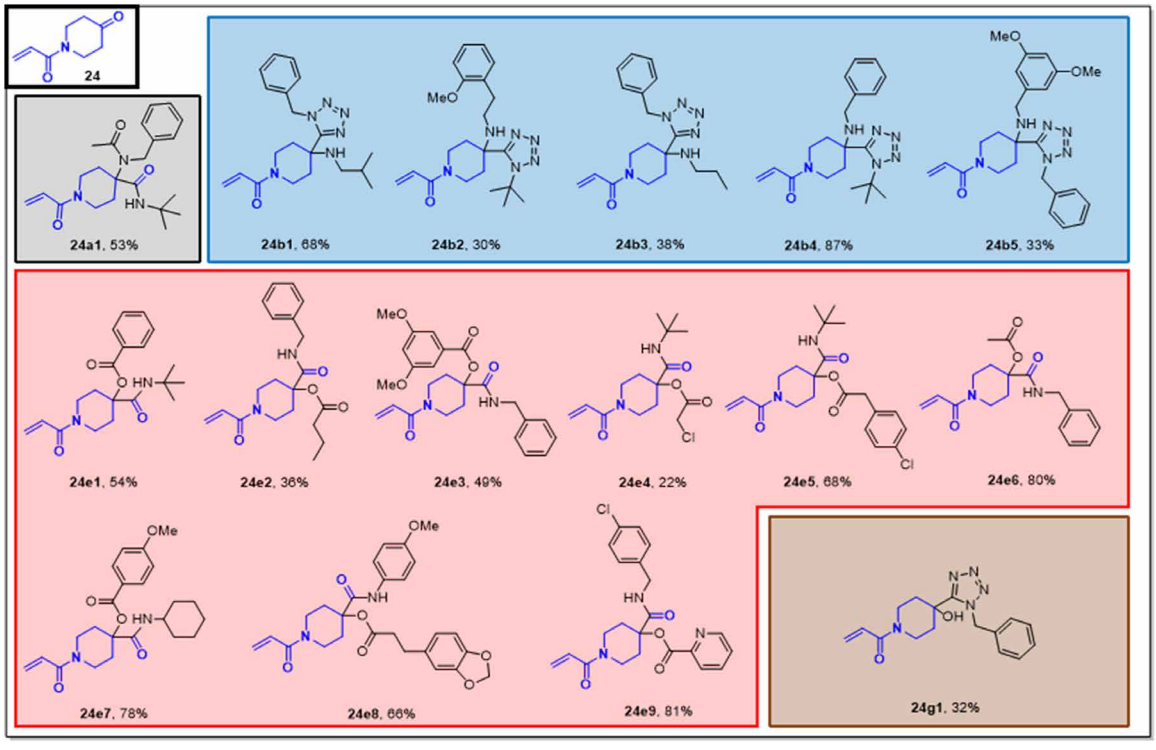

Fig. 6. Millimole-scale synthesis of electrophiles based on acrylamide ketone building block 24. The color of the boxes refers to the scaffolds shown in Table 1.

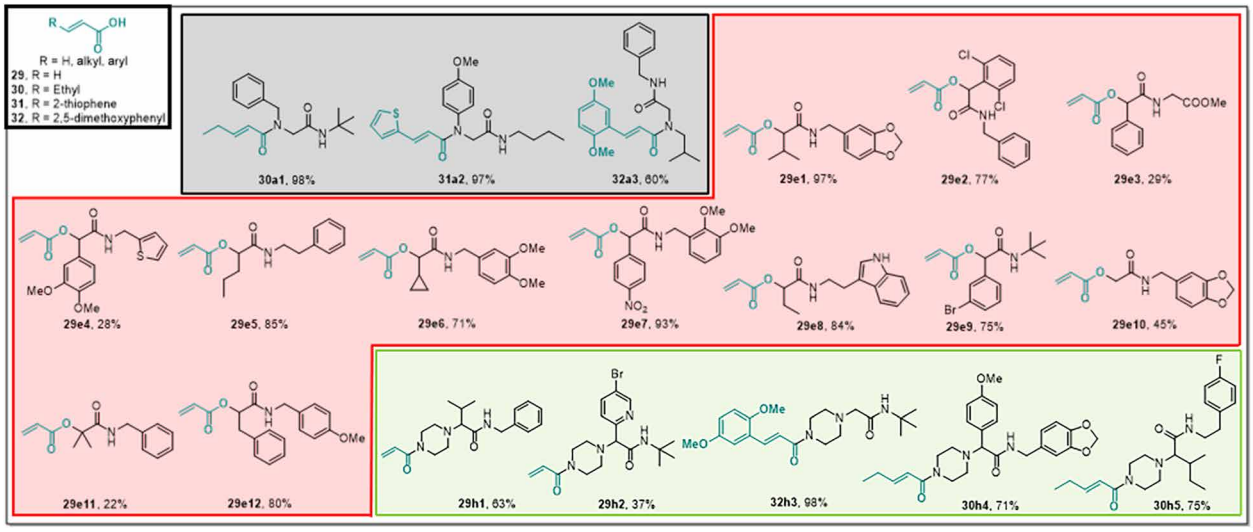

Fig. 7. Millimole-scale synthesis of electrophiles based on acrylic acid building blocks 29 to 32. The color of the boxes refers to the scaffolds shown in Table 1.

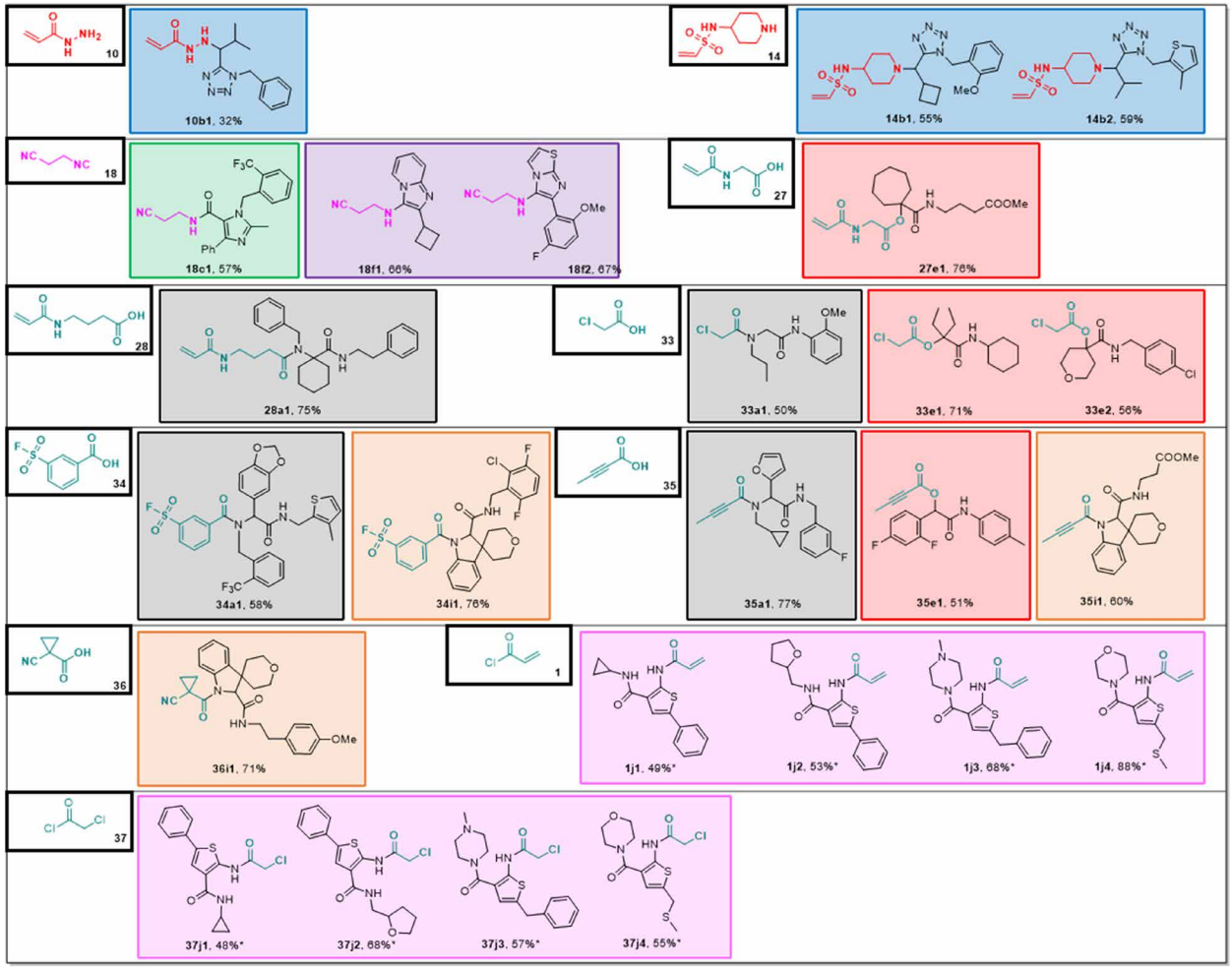

Fig. 8. Millimole-scale synthesis of electrophiles based on singleton building blocks 10, 14, 18, 27, 28, and 33 to 37 (*yield over two steps). Boxed color code is according to scaffold type of Table 1.

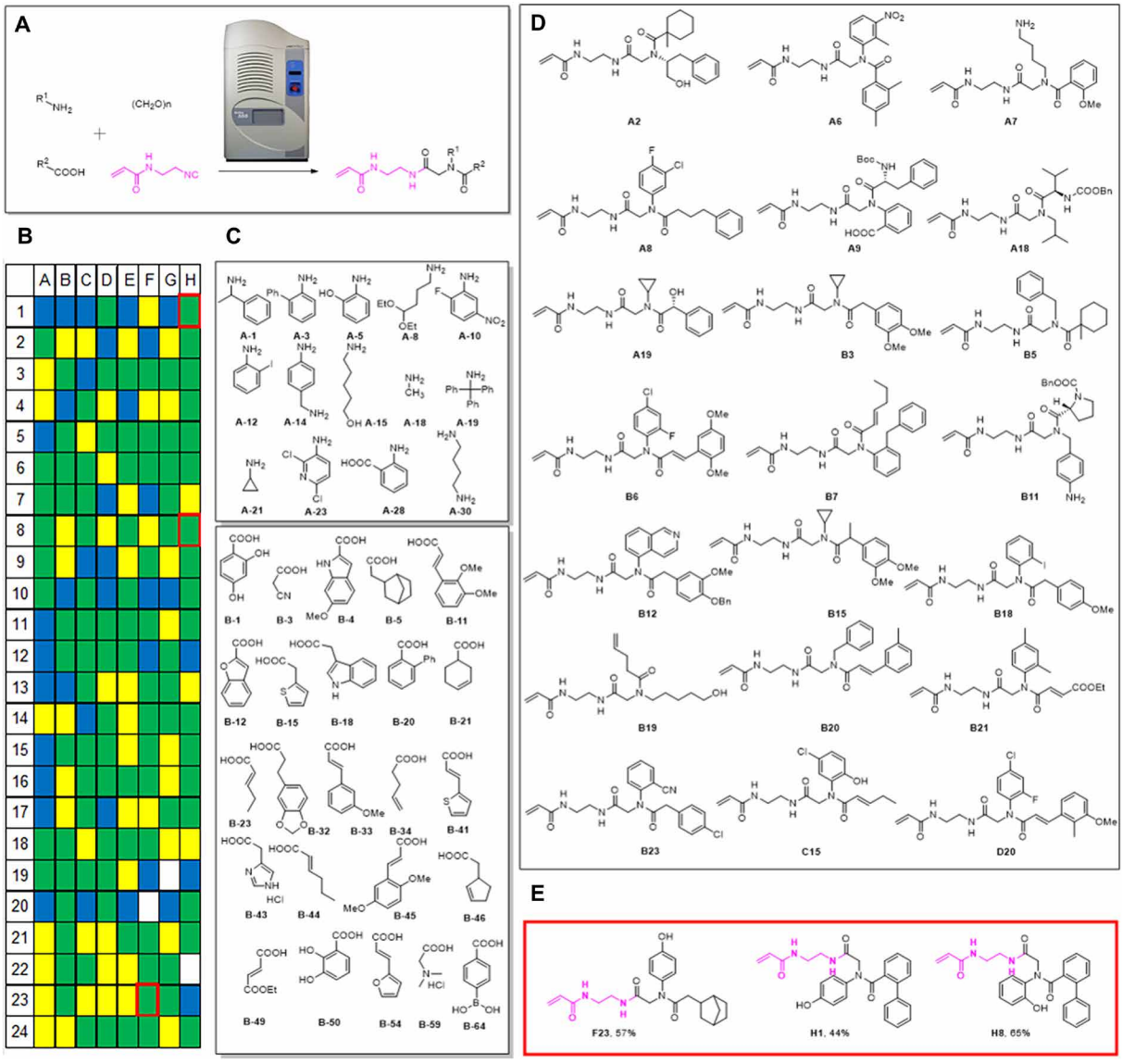

Fig. 9. Automated nanoscale synthesis of acrylamides using ADE. (**A**) ADE-enabled nanoscale automated electrophile synthesis based on the U-4CR of isocyanide building block **22**. (**B**) Heat plot of 192 compounds based on mass spectrometry analysis: green for major product formation, yellow for medium product formation, blue for no product formation, and white for Echo reagent transfer failure. (**C**) Exemplary amine and carboxylic acid building blocks used. (**D**) Exemplary product structures of the first two columns A and B. (**E**) Structures of resynthesized compounds on a millimole scale (red-boxed in heat plot).

8). Ethylenediamine-derived building block **6** was introduced in five different Ugi four-component reactions (U-4CRs) (Table 1, **a**) with an average yield of 50% (Fig. 4). Moreover, we synthesized four highly substituted α-amino tetrazoles with an average yield of 63%. Substituted and unsubstituted aromatic, aliphatic, and alicyclic reagents worked well to satisfying. We also incorporated **6** into a flat heterocyclic imidazole scaffold, which can be accessed in two steps via an Ugi reaction followed by cyclization (**6c1** and **6c2**; Table 1, **c**) as well as into three imino-hydantoin examples (**6d1** to **6d3**; Table 1, **d**). The functional group compatibility of screening compounds is of high importance as it increases the chance to capture interactions with the receptors.

Building block **22** is an ethylenediamine-derived acrylamide isocyanide and was synthesized in a three-step sequence on a gram scale (Fig. 3). The isocyanide was introduced in two variations of the Ugi reaction [U-4CR and Ugi tetrazole four-component reaction (UT-4CR)] as well as two variations of the Passerini reaction [Passerini three-component reaction (P-3CR) and Passerini tetrazole three component reaction (PT-3CR)]. In total, 24 derivatives were produced in an average of 75% yield (Fig. 5). Bis-allylamine (**22b13**) and bromo phenyl (**22b7**, **22e7**, and **22e8**) compounds could be further reacted, for example, by an ring-closing metathesis or Pd-catalyzed cross-coupling reactions (e.g., Suzuki-Miyaura reaction).

The oxopiperidine *N*-acrylate building block **24** was introduced in four different scaffolds including U-4CR, P-3CR, PT-3CR, and UT-4CR (Table 1), in 16 different examples in an average yield of 55% (Fig. 6). Compound **24g1**, for example, can be synthesized from simple building blocks in one step involving a newly described Passerini tetrazole reaction in 32% isolated yields (*37*).

Next, we evaluated the reactivity of acrylic acid and several derivatives thereof (Fig. 7). Substituted acrylates have been used to fine-tune

the reactivity toward nucleophiles (*44*). Four different acrylic acid derivatives have been used here in the U-4CR, the P-3CR, and the split U-4CR to yield 20 compounds at an average yield of 69%.

Last, we scouted other building blocks to increase the structural diversity of the electrophile library by performing singleton or small number syntheses (Fig. 8). In the UT-4CR, not only primary and secondary amines but also acryl hydrazones reacted smoothly. Thus, we synthesized acryl hydrazone building block **10** (Fig. 3) and reacted it in the UT-4CR to yield acrylhydrazone tetrazole **10b1**. Vinyl sulfonamide building block **14** was combined similarly in the UT-4CR, yielding the reactive vinyl sulfonamide electrophiles (**14b1** and **14b2**). Arylsulfonylfluorides were described as privileged warheads in chemical biology with the right balance of biocompatibility and protein reactivity, modifying not only reactive serines but also context-specific threonine, lysine, tyrosine, cysteine, and histidine residues (*45*). The cyano group is not only a potent electrophile but the β-cyanoethyl group was recently also described as a protecting group to yield *N*-unsubstituted tetrazoles (*42*, *46*). β-Cyanoethyl isocyanide **18** was introduced in different heterocyclic rings including imidazole (**18c1**), imidazopyridine (**18f1**), and imidazothiazole (**18f2**). Glycine-*N*-acrylate **27** and 4-amino butanoic acid *N*-acrylate **28** are examples of amino acid building blocks. Chloroacetic acid **33** works well in the Ugi and Passerini reactions and provides straightforward access to libraries of diversified chloroacetates, e.g., **33a1** and **33e1** and **33e2**. Arylsulfonylfluoride building block **34** was reacted as a carboxylic acid in an U-4CR yielding **34a1** in 58% isolated yield or to the spirocycle **34i1** in 76% yield. Worthwhile to mention is the water-solubilizing tetrahydropyrane ring in **34i1**. Butinyl carboxylic acid **35** yielded Ugi product **35a1**, Passerini product **35e1**, and spirocycle **35i1** in moderate to good yield. α-Cyanocyclopropyl carboxylic acid **36** yielded spirocycle **36i1**. The α-cyano cyclopropyl moiety can often be found in reversible cysteine protease inhibitors (*47*). Acrylic acid chloride **1**, and chloroacetyl chloride **37**, were used for the late-stage functionalization of 2-amino thiophenes produced by a Gewald three-component reaction (GW-3CR; **1j1** to **1j4** and **37j1** to **37j4**) (*41*).

Nanoscale synthesis

Automated, accelerated, nanoscale synthesis of compound libraries for the purpose of reaction evaluation and screening for biologically active compounds recently became an important alternative to manual macroscopic syntheses (*40*, *48*–*54*). Nanoscale synthesis not only allows for fast and automated production of large compound collections but also is highly sustainable as much fewer valuable reagents, solvent, and consumables are used (*55*). We have recently introduced acoustic droplet ejection (ADE) as a suitable tool for the automated nanoscale synthesis of libraries of small molecules (*40*, *48*, *54*). Here, we describe the Ugi-4CR of carboxylic acids, primary amines, formaldehyde, and *N*-(2-isocyanoethyl)acrylamide **22** as an example for the nanoscale synthesis of electrophiles for potential covalent biological space scouting. We chose formaldehyde as a constant component because the methylene group renders the compounds more flexible as opposed to the Ugi scaffold incorporating substituted aldehydes and ketones. The nanosynthesis was performed as recently described by us (Supplementary Materials) (*40*, *48*, *54*). In brief, we used stock solutions of the appropriate building block carboxylic acids, formaldehyde, amines, and *N*-(2-isocyanoethyl)acrylamide **22** in ethylene glycol or 2-methoxy ethanol depending on solubility as 0.5 M stock solutions in 384-well source plates. The building blocks were automatically transferred into 384-well destination plates using an Echo 555 instrument. From each building block, 750 nl was sequentially transferred. The transfer time to charge one 384-well plate was ~150 min. The plates were then covered with a sealing foil and shaken for 24 hours. Then, the plates were unsealed and each well was diluted with 100 μl of ethylene glycol. The reactions were analyzed by direct injection into a mass spectrometer as recently described (*40*, *48*, *54*). The heights of the molecular ion peak or that of a derivative served to create a crude reaction classifier. The analytical outcome of the reaction is shown in Fig. 9. Of the 192 reactions, 53% gave the expected compound as a major product (depicted in green), while 20% of the reactions give no product at all (depicted in blue). In total, four 384-well plates were created, potentially yielding 1536 electrophiles. Noteworthy is the building block diversity used to assemble this array of electrophiles and some exemplary products are shown in Fig. 9. We used building blocks with two differentially reactive amines, an aniline and a benzylamine (**A-14**), *o*-amino phenol (**A-5**), *o*-amino-biphenyl (**A-3**), bulky trityl amine (**A-19**) and small methyl (**A-18**) or isopropylamine (**A-21**), or symmetrical butane 1,4-diamine (**A-30**) which can react mono or bis, highly substituted pyridyl-3-amine (**A-23**) that can undergo further nucleophilic aromatic substitution reactions, anthranilic acid (**A-28**), and pentane-5-olamine (**A-15**). Different benzoic acid building blocks were introduced, including phenol (**B-1**, **B-50**), boronic acid (**B-64**), *o*-biphenyl (**B-20**), and α,β-unsaturated carboxylic acids (**B-23**, **B-33**, **B-41**, **B-44**, **B-45**, **B-49**, and **B-54**). Especially worthwhile to mention is maleic acid derivative (**B-49**) which can undergo further addition reactions (*56*). A great diversity of heterocyclic building blocks was introduced, e.g., thiophene (**B-15**), benzofuran (**B-12**), indole (**B-4**, **B-18**), imidazole (**B-43**), furan (**B-54**), and cyanoacetic acid (**B-3**). Exemplary reaction products are also shown in Fig. 9, for example, the constrained proline derivative (**B11**) or isoquinoline derivative (**B12**). Other products include a diversity of unprotected functional groups such as aliphatic hydroxy (**A2**, **A19**, and **B19**), phenol (**C15**), amino group (**A7** and **B11**), Boc-protected amine, and free carboxylic acid group (**A9**). **B6**, **B7**, **B20**, **B21**, **C15**, and **D20** are examples of *bis*-α,β-unsaturated carbonyl scaffolds. Last, we resynthesized some of the library compounds out for the plates to confirm scalability and provide full analytical data and yields. The three products are **F23** (57%), **H1** (44%), and **H9** (65%) and feature biphenyl, *o*-, and *p*-phenol as interesting structural moieties. In summary, the ADE-enabled nanoscale synthesis of electrophiles allows for the rapid and automated assembly of a diverse functional group and shape rich chemical space.

Covalent libraries are of great use in biology and drug discovery. The potential of electrophile (-fragment) screening as a practical and efficient tool for covalent-ligand discovery is well described (*25*). Few generalized approaches toward covalent libraries have been described while the need for biological screening of electrophiles is increasing (*24*, *25*, *57*, *58*). The strategic formation of covalent bonds between small molecules and proteins has many other underappreciated applications as enabling platforms for drug discovery (*59*). For example, targeting of noncatalytic cysteine residues in an allele-specific manner with small molecules is drawing attention from drug discovery scientists and chemical biologists (*27*). Acquired cysteines in cancer can be targeted by covalent inhibitors and several clinical trials are under way (*60*), whereas reactive-cysteine profiling for drug discovery has been described in a proteome-wide scale (*26*). However, the construction of diverse libraries of electrophiles is

challenging, and general access is demanding and underexplored. Therefore, we report here a holistic covalent library synthesis approach. The greatest advantage of our approach is the simple one-pot synthesis of electrophiles instead of sequential multistep synthesis, and as an example, we exercised the approach with 10 different scaffolds. The MCRs allow for the exploration of a very large chemical space based on a great number of archetypical commercially available building blocks such as primary amines, carboxylic acids, and aldehydes. For this, we synthesized nine different bifunctional building blocks on a gram scale or used commercially available building blocks incorporating an electrophile, a linker and an orthogonal MCR-compatible functional group (e.g., isocyanide, carbocyclic acid, and amine). These different electrophile building blocks were introduced in 10 different scaffolds. The generality and usefulness of our approach are reflected in the compatibility with many different functional groups, shapes, and electronic features. The generality of our approach is also reflected in the breath of scale from nanomole to millimole, the great number of synthesized compounds, and the diverse chemistries used. The syntheses were performed on a millimole scale, but also in an automated fashion on a nanoscale in 384- and 1536-well plate formats using ADE technology. Automated ADE-enabled chemistry allows the synthesis of tens of thousands of electrophiles. This methodology is amenable to a variety of MCRs as well as multiple classes of electrophile building blocks, allowing single-step access to a diverse array of products. Another benefit of the nanosynthesis is that any compound hitting a target during screening can be instantaneously resynthesized on a larger millimole scale for validation. One of the challenges of covalent library screening is that intrinsic reactivity of the warheads can vary greatly (*16*, *20*, *25*, *26*). However, a key advantage of our work is that, in many of our scaffold designs, the aliphatic linker between the warhead and main scaffold will normalize the intrinsic reactivity. Ongoing applications of our electrophile synthesis platform in our laboratory will be reported in due course.

MATERIALS AND METHODS

All reagents and solvents were purchased from Sigma-Aldrich, Abcr GmbH, Acros, Fluorochem, and AK Scientific and were used without further purification. All isocyanides were prepared in-house (see the Supplementary Materials). All microwave irradiation reactions were carried out in a Biotage Initiator Microwave Synthesizer. All sonication is performed in an ultrasonic cleaner (220/240 V, 25 A, and frequency of 50/60 Hz). Nuclear magnetic resonance (NMR) spectra were recorded on a Bruker AVANCE 500 spectrometer ^{1}H NMR (500 MHz) and ^{13}C NMR (126 MHz). Chemical shifts for ^{1}H NMR were reported as δ values, and coupling constants were in hertz (Hz). The following abbreviations were used for spin multiplicity: s = singlet, br s = broad singlet, d = doublet, br d = broad doublet, t = triplet, br t = broad triplet, q = quartet, dd = double of doublets, ddd = double of doublet of doublets, and m = multiplet. Chemical shifts for ^{13}C NMR reported in parts per million relative to the solvent peak. Thin-layer chromatography was performed using precoated silica gel 60 F_{254} plates (Merck, Darmstadt), and the spots were visualized with ultraviolet light at 254 nm. Flash chromatography was performed on a Reveleris X2 Flash Chromatography, using Grace Reveleris Silica flash cartridges (12 g). Mass spectra were measured on a Waters Investigator Supercritical Fluid Chromatograph with a 3100 Mass Detector (electrospray ionization) using a solvent system of methanol and CO_2 on a Viridis silica gel column (4.6 × 250 mm, 5-μm particle size) or Viridis 2-ethyl pyridine column (4.6 × 250 mm, 5-μm particle size). High-resolution mass spectra were recorded using a LTQ-Orbitrap-Velos Pro (Thermo Fisher Scientific) in ESI-positive mode at a resolution of 60000 at m/z 400.

SUPPLEMENTARY MATERIALS

Supplementary material for this article is available at http://advances.sciencemag.org/cgi/content/full/7/6/eabd9307/DC1

View/request a protocol for this paper from *Bio-protocol*.

REFERENCES AND NOTES

1. R. Lagoutte, N. Winssinger, Following the lead from nature with covalent inhibitors. *Chimia* **71**, 703–711 (2017).
2. J. G. Robertson, Enzymes as a special class of therapeutic target: Clinical drugs and modes of action. *Curr. Opin. Struct. Biol.* **17**, 674–679 (2007).
3. Y. Guo, Y. Liu, N. Hu, D. Yu, C. Zhou, G. Shi, B. Zhang, M. Wei, J. Liu, L. Luo, Z. Tang, H. Song, Y. Guo, X. Liu, D. Su, S. Zhang, X. Song, X. Zhou, Y. Hong, S. Chen, Z. Cheng, S. Young, Q. Wei, H. Wang, Q. Wang, L. Lv, F. Wang, H. Xu, H. Sun, H. Xing, N. Li, W. Zhang, Z. Wang, G. Liu, Z. Sun, D. Zhou, W. Li, L. Liu, L. Wang, Z. Wang, Discovery of Zanubrutinib (BGB-3111), a novel, potent, and selective covalent inhibitor of bruton's tyrosine kinase. *J. Med. Chem.* **62**, 7923–7940 (2019).
4. J. Canon, K. Rex, A. Y. Saiki, C. Mohr, K. Cooke, D. Bagal, K. Gaida, T. Holt, C. G. Knutson, N. Koppada, B. A. Lanman, J. Werner, A. S. Rapaport, T. S. Miguel, R. Ortiz, T. Osgood, J.-R. Sun, X. Zhu, J. D. McCarter, L. P. Volak, B. E. Houk, M. G. Fakih, B. H. O'Neil, T. J. Price, G. S. Falchook, J. Desai, J. Kuo, R. Govindan, D. S. Hong, W. Ouyang, H. Henary, T. Arvedson, V. J. Cee, J. R. Lipford, The clinical KRAS(G12C) inhibitor AMG 510 drives anti-tumour immunity. *Nature* **575**, 217–223 (2019).
5. F. A. Balaguer, T. Mühlethaler, J. Estévez-Gallego, E. Calvo, J. F. Giménez-Abián, A. L. Risinger, E. J. Sorensen, C. D. Vanderwal, K. -H. Altmann, S. L. Mooberry, M. O. Steinmetz, M. Á. Oliva, A. E. Prota, J. F. Díaz, Crystal structure of the cyclostreptin-tubulin adduct: Implications for tubulin activation by taxane-site ligands. *Int. J. Mol. Sci.* **20**, 1392 (2019).
6. A. J. T. Smith, X. Zhang, A. G. Leach, K. N. Houk, Beyond picomolar affinities: Quantitative aspects of noncovalent and covalent binding of drugs to proteins. *J. Med. Chem.* **52**, 225–233 (2009).
7. D. S. Johnson, E. Weerapana, B. F. Cravatt, Strategies for discovering and derisking covalent, irreversible enzyme inhibitors. *Future Med. Chem.* **2**, 949–964 (2010).
8. T. A. Baillie, Targeted covalent inhibitors for drug design. *Angew. Chem. Int. Ed.* **55**, 13408–13421 (2016).
9. K. M. Backus, B. E. Correia, K. M. Lum, S. Forli, B. D. Horning, G. E. González-Páez, S. Chatterjee, B. R. Lanning, J. R. Teijaro, A. J. Olson, D. W. Wolan, B. F. Cravatt, Proteome-wide covalent ligand discovery in native biological systems. *Nature* **534**, 570–574 (2016).
10. Y. Yamashita, E. Vinogradova, X. Zhang, R. Suciu, B. Cravatt, A chemical proteomic probe for the mitochondrial pyruvate carrier complex. *Angew. Chem. Int. Ed.* **59**, 3896–3899 (2020).
11. A. Chaikuad, P. Koch, S. A. Laufer, S. Knapp, The cysteinome of protein kinases as a target in drug development. *Angew. Chem. Int. Ed.* **57**, 4372–4385 (2018).
12. P. Martín-Gago, E. K. Fansa, M. Winzker, S. Murarka, P. Janning, C. Schultz-Fademrecht, M. Baumann, A. Wittinghofer, H. Waldmann, Covalent protein labeling at glutamic acids. *Cell Chem. Biol.* **24**, 589–597.e5 (2017).
13. D. A. E. Cross, S. E. Ashton, S. Ghiorghiu, C. Eberlein, C. A. Nebhan, P. J. Spitzler, J. P. Orme, M. R. V. Finlay, R. A. Ward, M. J. Mellor, G. Hughes, A. Rahi, V. N. Jacobs, M. R. Brewer, E. Ichihara, J. Sun, H. Jin, P. Ballard, K. Al-Kadhimi, R. Rowlinson, T. Klinowska, G. H. P. Richmond, M. Cantarini, D.-W. Kim, M. R. Ranson, W. Pao, AZD9291, an Irreversible EGFR TKI, overcomes T790M-mediated resistance to EGFR inhibitors in lung cancer. *Cancer Discov.* **4**, 1046–1061 (2014).
14. Q. Zheng, J. L. Woehl, S. Kitamura, D. Santos-Martins, C. J. Smedley, G. Li, S. Forli, J. E. Moses, D. W. Wolan, K. B. Sharpless, SuFEx-enabled, agnostic discovery of covalent inhibitors of human neutrophil elastase. *Proc. Natl. Acad. Sci. U.S.A.* **116**, 18808–18814 (2019).
15. I. W. Windsor, M. J. Palte, J. C. Lukesh, B. Gold, K. T. Forest, R. T. Raines, Sub-picomolar inhibition of HIV-1 protease with a boronic acid. *J. Am. Chem. Soc.* **140**, 14015–14018 (2018).
16. A. Douangamath, D. Fearon, P. Gehrtz, T. Krojer, P. Lukacik, C. D. Owen, E. Resnick, C. Strain-Damerell, A. Aimon, P. Ábrányi-Balogh, J. Brandão-Neto, A. Carbery, G. Davison, A. Dias, T. D. Downes, L. Dunnett, M. Fairhead, J. D. Firth, S. P. Jones, A. Keeley, G. M. Keserü, H. F. Klein, M. P. Martin, M. E. M. Noble, P. O'Brien, A. Powell, R. N. Reddi,

R. Skyner, M. Snee, M. J. Waring, C. Wild, N. London, F. von Delft, M. A. Walsh, Crystallographic and electrophilic fragment screening of the SARS-CoV-2 main protease. *Nat. Commun.* **11**, 5047 (2020).
17. D. J. Augeri, J. A. Robl, D. A. Betebenner, D. R. Magnin, A. Khanna, J. G. Robertson, A. Wang, L. M. Simpkins, P. Taunk, Q. Huang, S.-P. Han, B. Abboa-Offei, M. Cap, L. Xin, L. Tao, E. Tozzo, G. E. Welzel, D. M. Egan, J. Marcinkeviciene, S. Y. Chang, S. A. Biller, M. S. Kirby, R. A. Parker, L. G. Hamann, Discovery and preclinical profile of saxagliptin (BMS-477118): A highly potent, long-acting, orally active dipeptidyl peptidase IV inhibitor for the treatment of type 2 diabetes. *J. Med. Chem.* **48**, 5025–5037 (2005).
18. U. P. Dahal, A. M. Gilbert, R. S. Obach, M. E. Flanagan, J. M. Chen, C. Garcia-Irizarry, J. T. Starr, B. Schuff, D. P. Uccello, J. A. Young, Intrinsic reactivity profile of electrophilic moieties to guide covalent drug design: *N*-α-acetyl-l-lysine as an amine nucleophile. *MedChemComm* **7**, 864–872 (2016).
19. D. A. Erlanson, A. C. Braisted, D. R. Raphael, M. Randal, R. M. Stroud, E. M. Gordon, J. A. Wells, Site-directed ligand discovery. *Proc. Natl. Acad. Sci. U.S.A.* **97**, 9367–9372 (2000).
20. J. S. Martin, C. J. MacKenzie, D. Fletcher, I. H. Gilbert, Characterising covalent warhead reactivity. *Bioorg. Med. Chem.* **27**, 2066–2074 (2019).
21. G. B. Craven, D. P. Affron, C. E. Allen, S. Matthies, J. G. Greener, R. M. L. Morgan, E. W. Tate, A. Armstrong, D. J. Mann, High-throughput kinetic analysis for target-directed covalent ligand discovery. *Angew. Chem. Int. Ed.* **57**, 5257–5261 (2018).
22. A. Keeley, P. Ábrányi-Balogh, G. M. Keserű, Design and characterization of a heterocyclic electrophilic fragment library for the discovery of cysteine-targeted covalent inhibitors. *MedChemComm* **10**, 263–267 (2019).
23. S. G. Kathman, Z. Xu, A. V. Statsyuk, A fragment-based method to discover irreversible covalent inhibitors of cysteine proteases. *J. Med. Chem.* **57**, 4969–4974 (2014).
24. C. E. Allen, P. R. Curran, A. S. Brearley, V. Boissel, L. Sviridenko, N. J. Press, J. P. Stonehouse, A. Armstrong, Efficient and facile synthesis of acrylamide libraries for protein-guided tethering. *Org. Lett.* **17**, 458–460 (2015).
25. E. Resnick, A. Bradley, J. Gan, A. Douangamath, T. Krojer, R. Sethi, P. P. Geurink, A. Aimon, G. Amitai, D. Bellini, J. Bennett, M. Fairhead, O. Fedorov, R. Gabizon, J. Gan, J. Guo, A. Plotnikov, N. Reznik, G. F. Ruda, L. Díaz-Sáez, V. M. Straub, T. Szommer, S. Velupillai, D. Zaidman, Y. Zhang, A. R. Coker, C. G. Dowson, H. M. Barr, C. Wang, K. V. M. Huber, P. E. Brennan, H. Ovaa, F. von Delft, N. London, Rapid covalent-probe discovery by electrophile-fragment screening. *J. Am. Chem. Soc.* **141**, 8951–8968 (2019).
26. A. J. Maurais, E. Weerapana, Reactive-cysteine profiling for drug discovery. *Curr. Opin. Chem. Biol.* **50**, 29–36 (2019).
27. K. K. Hallenbeck, D. M. Turner, A. R. Renslo, M. R. Arkin, Targeting non-catalytic cysteine residues through structure-guided drug discovery. *Curr. Top. Med. Chem.* **17**, 4–15 (2017).
28. J. Baell, M. A. Walters, Chemistry: Chemical con artists foil drug discovery. *Nature* **513**, 481–483 (2014).
29. J. B. Baell, G. A. Holloway, New substructure filters for removal of pan assay interference compounds (PAINS) from screening libraries and for their exclusion in bioassays. *J. Med. Chem.* **53**, 2719–2740 (2010).
30. I. Ugi, The α-addition of immonium ions and anions to isonitriles accompanied by secondary reactions. *Angew. Chem. Int. Ed.* **1**, 8–21 (1962).
31. C. G. Neochoritis, T. Zhao, A. Dömling, Tetrazoles via Multicomponent Reactions. *Chem. Rev.* **119**, 1970–2042 (2019).
32. R. Madhavachary, T. Zarganes-Tzitzikas, P. Patil, K. Kurpiewska, J. Kalinowska-Tłuścik, A. Dömling, Synthesis of highly substituted imidazole uracil containing molecules via Ugi-4CR and Passerini-3CR. *ACS Comb. Sci.* **20**, 192–196 (2018).
33. I. Ugi, F. K. Rosendahl, F. Bodesheim, Isonitrile, XIII. Kondensation von primären Aminen und Ketonen mit Isonitrilen und Rhodanwasserstoffsäure. *Liebigs Ann.* **666**, 54–61 (1963).
34. M. Passerini, L. Simone, Sopra gli isonitrili (I). Composto del p-isonitril-azobenzolo con acetone ed acido acetico. *Gazz. Chim. Ital* **51**, 126–129 (1921).
35. H. Bienaymé, K. Bouzid, A new heterocyclic multicomponent reaction for the combinatorial synthesis of fused 3-aminoimidazoles. *Angew. Chem. Int. Ed.* **37**, 2234–2237 (1998).
36. A. Boltjes, A. Dömling, The groebke-blackburn-bienaymé reaction. *Eur. J. Org. Chem.* **2019**, 7007–7049 (2019).
37. A. L. Chandgude, A. Dömling, An efficient Passerini tetrazole reaction (PT-3CR). *Green Chem.* **18**, 3718–3721 (2016).
38. I. Ugi, R. Meyr, Isonitrile, V. erweiterter anwendungsbereich der passerini-reaktion. *Chem. Ber.* **94**, 2229–2233 (1961).
39. G. B. Giovenzana, G. C. Tron, S. Di Paola, I. G. Menegotto, T. Pirali, A mimicry of primary amines by bis-secondary diamines as components in the ugi four-component reaction. *Angew. Chem. Int. Ed.* **45**, 1099–1102 (2006).
40. S. Shaabani, R. Xu, M. Ahmadianmoghaddam, L. Gao, M. Stahorsky, J. Olechno, R. Ellson, M. Kossenjans, V. Helan, A. Dömling, Automated and accelerated synthesis of indole derivatives on a nano-scale. *Green Chem.* **21**, 225–232 (2019).
41. K. Wang, D. Kim, A. Dömling, Cyanoacetamide MCR (III): Three-component gewald reactions revisited. *J. Comb. Chem.* **12**, 111–118 (2010).
42. E. Kroon, K. Kurpiewska, J. Kalinowska-Tłuścik, A. Dömling, Cleavable β-cyanoethyl isocyanide in the ugi tetrazole reaction. *Org. Lett.* **18**, 4762–4765 (2016).
43. S. H. Watterson, Q. Liu, M. B. Bertrand, D. G. Batt, L. Li, M. A. Pattoli, S. Skala, L. Cheng, M. T. Obermeier, R. Moore, Z. Yang, R. Vickery, P. A. Elzinga, L. Discenza, C. D'Arienzo, K. M. Gillooly, T. L. Taylor, C. Pulicicchio, Y. Zhang, E. Heimrich, K. W. McIntyre, Q. Ruan, R. A. Westhouse, I. M. Catlett, N. Zheng, C. Chaudhry, J. Dai, M. A. Galella, A. J. Tebben, M. Pokross, J. Li, R. Zhao, D. Smith, R. Rampulla, A. Allentoff, M. A. Wallace, A. Mathur, L. Salter-Cid, J. E. Macor, P. H. Carter, A. Fura, J. R. Burke, J. A. Tino, Discovery of Branebrutinib (BMS-986195): A strategy for identifying a highly potent and selective covalent inhibitor providing rapid in vivo inactivation of Bruton's Tyrosine Kinase (BTK). *J. Med. Chem.* **62**, 3228–3250 (2019).
44. S. Xu, A. Aguilar, L. Huang, T. Xu, K. Zheng, D. M. Eachern, S. Przybranowski, C. Foster, K. Zawacki, Z. Liu, K. Chinnaswamy, J. Stuckey, S. Wang, Discovery of M-808 as a highly potent, covalent, small-molecule inhibitor of the Menin–MLL interaction with strong *In Vivo* antitumor activity. *J. Med. Chem.* **63**, 4997–5010 (2020).
45. A. Narayanan, L. H. Jones, Sulfonyl fluorides as privileged warheads in chemical biology. *Chem. Sci.* **6**, 2650–2659 (2015).
46. A. Boltjes, A. Shrinidhi, K. van de Kolk, E. Herdtweck, A. Dömling, Gd-TEMDO: Design, synthesis, and MRI application. *Chem. A Eur. J.* **22**, 7352–7356 (2016).
47. L. Cianni, G. Sartori, F. Rosini, D. De Vita, G. Pires, B. R. Lopes, A. Leitão, A. C. B. Burtoloso, C. A. Montanari, Leveraging the cruzain S3 subsite to increase affinity for reversible covalent inhibitors. *Bioorg. Chem.* **79**, 285–292 (2018).
48. Y. Wang, S. Shaabani, M. Ahmadianmoghaddam, L. Gao, R. Xu, K. Kurpiewska, J. Kalinowska-Tluscik, J. Olechno, R. Ellson, M. Kossenjans, V. Helan, M. Groves, A. Dömling, Acoustic droplet ejection enabled automated reaction scouting. *ACS Cent. Sci.* **5**, 451–457 (2019).
49. S. M. Mennen, C. Alhambra, C. L. Allen, M. Barberis, S. Berritt, T. A. Brandt, A. D. Campbell, J. Castañón, A. H. Cherney, M. Christensen, D. B. Damon, J. E. de Diego, S. García-Cerrada, P. García-Losada, R. Haro, J. Janey, D. C. Leitch, L. Li, F. Liu, P. C. Lobben, D. W. C. MacMillan, J. Magano, E. M. Inturff, S. Monfette, R. J. Post, D. Schultz, B. J. Sitter, J. M. Stevens, I. I. Strambeanu, J. Twilton, K. Wang, M. A. Zajac, The evolution of high-throughput experimentation in pharmaceutical development and perspectives on the future. *Org. Process Res. Dev.* **23**, 1213–1242 (2019).
50. S. Lin, S. Dikler, W. D. Blincoe, R. D. Ferguson, R. P. Sheridan, Z. Peng, D. V. Conway, K. Zawatzky, H. Wang, T. Cernak, I. W. Davies, D. A. Di Rocco, H. Sheng, C. J. Welch, S. D. Dreher, Mapping the dark space of chemical reactions with extended nanomole synthesis and MALDI-TOF MS. *Science* **361**, eaar6236 (2018).
51. M. Benz, M. R. Molla, A. Böser, A. Rosenfeld, P. A. Levkin, Marrying chemistry with biology by combining on-chip solution-based combinatorial synthesis and cellular screening. *Nat. Commun.* **10**, 2879 (2019).
52. T. Cernak, N. J. Gesmundo, K. Dykstra, Y. Yu, Z. Wu, Z.-C. Shi, P. Vachal, D. Sperbeck, S. He, B. A. Murphy, L. Sonatore, S. Williams, M. Madeira, A. Verras, M. Reiter, C. H. Lee, J. Cuff, E. C. Sherer, J. Kuethe, S. Goble, N. Perrotto, S. Pinto, D.-M. Shen, R. Nargund, J. Balkovec, R. J. De Vita, S. D. Dreher, Microscale high-throughput experimentation as an enabling technology in drug discovery: Application in the discovery of (Piperidinyl) pyridinyl-1 *H*-benzimidazole diacylglycerol acyltransferase 1 inhibitors. *J. Med. Chem.* **60**, 3594–3605 (2017).
53. A. B. Santanilla, E. L. Regalado, T. Pereira, M. Shevlin, K. Bateman, L.-C. Campeau, J. Schneeweis, S. Berritt, Z.-C. Shi, P. Nantermet, Y. Liu, R. Helmy, C. J. Welch, P. Vachal, I. W. Davies, T. Cernak, S. D. Dreher, Nanomole-scale high-throughput chemistry for the synthesis of complex molecules. *Science* **347**, 49–53 (2015).
54. C. G. Neochoritis, S. Shaabani, M. Ahmadianmoghaddam, T. Zarganes-Tzitzikas, L. Gao, M. Novotná, T. Mitríková, A. R. Romero, M. I. Irianti, R. Xu, J. Olechno, R. Ellson, V. Helan, M. Kossenjans, M. R. Groves, A. Dömling, Rapid approach to complex boronic acids. *Sci. Adv.* **5**, eaaw4607 (2019).
55. H. Wong, T. Cernak, Reaction miniaturization in eco-friendly solvents. *Curr. Opin. Green Sustain. Chem.* **11**, 91–98 (2018).
56. X. Gao, C. Shan, Z. Chen, Y. Liu, X. Zhao, A. Zhang, P. Yu, H. Galons, Y. Lan, K. Lu, One-pot synthesis of β-lactams by the Ugi and Michael addition cascade reaction. *Org. Biomol. Chem.* **16**, 6096–6105 (2018).
57. M. Pérez-Palau, J. Cornella, Synthesis of sulfonyl fluorides from sulfonamides. *Eur. J. Org. Chem.* , 2497–2500 (2020).
58. P. K. Chinthakindi, H. G. Kruger, T. Govender, T. Naicker, P. I. Arvidsson, On-water synthesis of biaryl sulfonyl fluorides. *J. Org. Chem.* **81**, 2618–2623 (2016).
59. S. E. Dalton, S. Campos, Covalent small molecules as enabling platforms for drug discovery. *Chembiochem* **21**, 1080–1100 (2019).
60. M. Visscher, M. R. Arkin, T. B. Dansen, Covalent targeting of acquired cysteines in cancer. *Curr. Opin. Chem. Biol.* **30**, 61–67 (2016).
61. R. Obrecht, R. Herrmann, I. Ugi, Isocyanide synthesis with phosphoryl chloride and diisopropylamine. *Synthesis* **1985**, 400–402 (1985).
62. G. Skorna, I. Ugi, Isocyanide synthesis with diphosgene. *Angew. Chem. Int. Ed.* **16**, 259–260 (1977).
63. I. Ugi, U. Fetzer, U. Eholzer, H. Knupfer, K. Offermann, Isonitrile syntheses. *Angew. Chem. Int. Ed.* **4**, 472–484 (1965).

64. I. Ugi, R. Meyr, o-Tolyl Isocyanide. *Organic Synth.* **41**, 101 (1961).
65. G. W. Gokel, R. P. Widera, W. P. Weber, Phase-transfer Hofmann carbylamine reaction: *Tert*-butyl isocyanide. *Organic Synth.* **55**, 96–96 (2003).
66. W. P. Weber, G. W. Gokel, I. K. Ugi, Phase transfer catalysis in the Hofmann carbylamine reaction. *Angew. Chem. Int. Ed.* **11**, 530–531 (1972).
67. C. G. Neochoritis, T. Zarganes-Tzitzikas, S. Stotani, A. Dömling, E. Herdtweck, K. Khoury, A. Dömling, Leuckart–Wallach route toward isocyanides and some applications. *ACS Comb. Sci.* **17**, 493–499 (2015).
68. Y. Huang, S. Wolf, M. Bista, L. Meireles, C. Camacho, T. A. Holak, A. Dömling, 1, 4-Thienodiazepine-2, 5-diones via MCR (I): Synthesis, virtual space and p53-Mdm2 activity. *Chem. Biol. Drug Des.* **76**, 116–129 (2010).
69. MarvinSketch was used for drawing of reaction; ChemAxon. www.chemaxon.com.
70. A. Osipyan, S. Shaabani, R. Warmerdam, S. V. Shishkina, H. Boltz, A. Dömling, Automated, accelerated nanoscale synthesis of iminopyrrolidines. *Angew. Chem. Int. Ed.* **59**, 12423–12427 (2020).
71. L. J. Hobson, W. J. Feast, Poly (amidoamine) hyperbranched systems: Synthesis, structure and characterization. *Polymer* **40**, 1279–1297 (1999).
72. J. M. Ostrem, U. Peters, M. L. Sos, J. A. Wells, K. M. Shokat, K-Ras (G12C) inhibitors allosterically control GTP affinity and effector interactions. *Nature* **503**, 548–551 (2013).
73. H. N. Pati, U. Das, J. W. Quail, M. Kawase, H. Sakagami, J. R. Dimmock, Cytotoxic 3, 5-bis (benzylidene) piperidin-4-ones and N-acyl analogs displaying selective toxicity for malignant cells. *Eur. J. Med. Chem.* **43**, 1–7 (2008).
74. C. Contino, J.-C. Maurizis, M. Ollier, M. Rapp, J.-M. Lacombe, B. Pucci, Synthesis of new cotelomers derived from tris (hydroxymethyl) aminomethane bearing arabinofuranosylcytosine moieties. Preliminary results on their in vitro and in vivo antitumoral activities. *Eur. J. Med. Chem.* **33**, 809–816 (1998).
75. R. Vroemans, F. Bamba, J. Winters, J. Thomas, J. Jacobs, L. Van Meervelt, J. John, W. Dehaen, Sequential Ugi reaction/base-induced ring closing/IAAC protocol toward triazolobenzodiazepine-fused diketopiperazines and hydantoins. *Beilstein J. Org. Chem.* **14**, 626–633 (2018).
76. V. Estévez, L. Kloeters, N. Kwietniewska, E. Vicente-García, E. Ruijter, R. V. A. Orru, Ugi-type reactions of spirocyclic indolenines as a platform for compound library generation. *Synlett* **28**, 376–380 (2017).
77. T. Lindhorst, H. Bock, I. Ugi, A new class of convertible isocyanides in the Ugi four-component reaction. *Tetrahedron* **55**, 7411–7420 (1999).

Acknowledgments
Funding: This research has been supported (to A.D.) by the National Institutes of Health (NIH) (2R01GM097082-05), the European Lead Factory (IMI) under grant agreement no. 115489, and the Qatar National Research Foundation (NPRP6-065-3-012). Moreover, funding was received through ITN "AcceleratedEarly stage drug dIScovery" (AEGIS, grant agreement no. 675555) and COFUND ALERT (grant agreement no. 665250), Hartstichting (eSCAPE-HF, 2018B012), and a KWF Kankerbestrijding grant (grant agreement no. 10504). F.S. acknowledges the LPDP (Indonesian Endowment Fund for Education) for support. S.S. acknowledges the KWF for financial support (grant agreement no. 10504). **Author contributions:** A.D. conceived and directed the project. S.S. and F.S. performed the HT synthesis of acryl amides using the building block approach with ADE technology. F.S., C.G.N., T.Z.-T., P.P., S.S., and E.G. synthesized the derivatives on a millimole scale. A.D. and S.S. cowrote the manuscript. **Competing interests:** The authors declare that they have no competing interests. **Data and materials availability:** All data needed to evaluate the conclusions in the paper are present in the paper and/or the Supplementary Materials. The herein described libraries can be obtained from us by interested laboratories through a collaboration.

Submitted 21 July 2020
Accepted 15 December 2020
Published 3 February 2021
10.1126/sciadv.abd9307

Citation: F. Sutanto, S. Shaabani, C. G. Neochoritis, T. Zarganes-Tzitzikas, P. Patil, E. Ghonchepour, A. Dömling, Multicomponent reaction–derived covalent inhibitor space. *Sci. Adv.* **7**, eabd9307 (2021).